

Activation of Skeletal Muscle Myosin Light Chain Kinase by Calcium(2+) and Calmodulin†

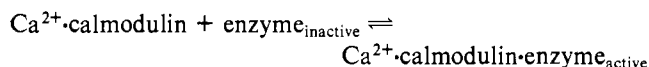
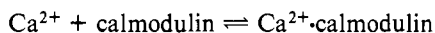
Donald K. Blumenthal* and James T. Stull

ABSTRACT: Many biological processes are now known to be regulated by Ca^{2+} via calmodulin (CM). Although a general mechanistic model by which Ca^{2+} and calmodulin modulate many of these activities has been proposed, an accurate quantitative model is not available. A detailed analysis of skeletal muscle myosin light chain kinase activation was undertaken in order to determine the stoichiometries and equilibrium constants of Ca^{2+} , calmodulin, and enzyme catalytic subunit in the activation process. The analysis indicates that activation is a sequential, fully reversible process requiring both Ca^{2+} and calmodulin. The first step of the activation process appears to require binding of Ca^{2+} to all four divalent metal binding sites on calmodulin to form the complex, Ca_4^{2+} -calmodulin. This complex then interacts with the inactive cat-

alytic subunit of the enzyme to form the active holoenzyme complex, Ca_4^{2+} -calmodulin-enzyme. Formation of the holoenzyme follows simple hyperbolic kinetics, indicating a 1:1 stoichiometry of Ca_4^{2+} -calmodulin to catalytic subunit. The rate equation derived from the mechanistic model was used to determine the values of $K_{\text{Ca}^{2+}}$ and K_{CM} , the intrinsic activation constants for each step of the activation process. $K_{\text{Ca}^{2+}}$ and K_{CM} were found to have values of 10 μM and 0.86 nM, respectively, at 10 mM Mg^{2+} . The rate equation using these equilibrium constants accurately predicts the extent of enzyme activation over a wide range of Ca^{2+} and calmodulin concentrations. The kinetic model and analytical techniques employed herein may be generally applicable to other enzymes with similar regulatory schemes.

M yosin light chain kinase, the enzyme catalyzing the phosphorylation of the phosphorylatable or P light chain of myosin, was first identified in fast-twitch skeletal muscle (Pires et al., 1974). The enzyme was subsequently purified to apparent homogeneity and shown to be a monomer of approximately 80 000 molecular weight (Pires & Perry, 1977; Yazawa & Yagi, 1978; Nairn & Perry, 1979). The purified enzyme specifically phosphorylated the P light chain of myosin, and was completely dependent on micromolar concentrations of Ca^{2+} (Pires et al., 1974; Pires & Perry, 1977). It was later shown that the activity of myosin light chain kinase from smooth muscle (Dabrowska et al., 1977), cardiac muscle (Walsh et al., 1979), and skeletal muscle (Yazawa & Yagi, 1977) was also dependent upon nanomolar concentrations of a small molecular weight protein, subsequently identified as calmodulin¹ (Barylko et al., 1978; Dabrowska et al., 1978; Yagi et al., 1978; Nairn & Perry, 1979). A wide variety of enzymes and cellular processes are now known to be regulated by calmodulin (recently reviewed by Cheung, 1980; Wolff & Brostrom, 1979; Wang & Waisman, 1979; Klee et al., 1980).

Activation of skeletal muscle myosin light chain kinase has been shown to follow a sequential, fully reversible activation scheme (Yazawa & Yagi, 1978) originally proposed for Ca^{2+} -dependent cyclic nucleotide phosphodiesterase (Teo & Wang, 1973; Lin et al., 1974; Brostrom & Wolff, 1974).



According to this general scheme, activation first requires the

formation of a Ca^{2+} -calmodulin complex which subsequently interacts with the inactive catalytic subunit to form a catalytically active holoenzyme.

Although this general scheme illustrates certain key features of the activation mechanism, it fails to provide quantitative information necessary for understanding the regulation of calmodulin-dependent processes in vivo. The purpose of the present study was a detailed analysis of the activation of skeletal muscle myosin light chain kinase by Ca^{2+} and calmodulin. From the kinetic analysis, a relatively simple mechanistic model is developed, including stoichiometries and equilibrium constants for Ca^{2+} , calmodulin, and enzyme catalytic subunit. An equation is derived capable of predicting the extent of enzyme activation over a wide range of Ca^{2+} and calmodulin concentrations. The techniques used for the analysis of myosin light chain kinase activation should be generally applicable to other calmodulin-dependent enzymes and processes.

Methods and Materials

Materials. DEAE-cellulose (DE-52) was purchased from Whatman, Ltd. Chelex-100 was obtained from Bio-Rad Laboratories. Cyanogen bromide activated Sepharose 4B was purchased from Sigma. Ultrapure magnesium salts were obtained from Alfa-Ventron Corp. and [γ -³²P]ATP was purchased from ICN Pharmaceuticals. All other chemicals were of analytical grade. All solutions were adjusted to the indicated pH values with HCl or NaOH.

Purification of Proteins. Mixed light chains used as substrates for myosin light chain kinase were prepared from fresh rabbit skeletal muscle and bovine ventricles. All procedures were carried out at 0–4 °C. Well-washed myofibrils were prepared as described by Solaro et al. (1971) and solubilized

† From the Moss Heart Center and the Department of Pharmacology, University of Texas Health Science Center, Dallas, Texas 75235. Received May 6, 1980. This work was supported by grants from NIH (HL23990) and the Muscular Dystrophy Association of America. D.K.B. was supported as a Predoctoral Trainee in the Division of Pharmacology at the University of California, San Diego (GM02267). A preliminary report of this work was presented at the 63rd Annual Meeting of the Federation of American Societies for Experimental Biology at Dallas, TX.

¹ Abbreviations used: CM, calmodulin, previously referred to as calcium-dependent regulator (CDR), modulator, and activator protein; EGTA, ethylene glycol bis(β -aminoethyl ether)-*N,N'*-tetraacetic acid; EDTA, (ethylenedinitrilo)tetraacetic acid; Mops, 3-(*N*-morpholino)-propanesulfonic acid; Tris, tris(hydroxymethyl)aminomethane.

in 8 M urea, 1 mM EDTA, 15 mM 2-mercaptoethanol, and 20 mM Tris, pH 8.0. To this solution was added an equal volume of 95% ethanol containing 15 mM 2-mercaptoethanol. The solution was stirred for 1 h to allow complete precipitation of protein before centrifuging at 8000g for 30 min. The precipitated protein was discarded. DEAE-cellulose was added to the supernatant fraction and mixed for at least 1 h before centrifugation at 200g for 10 min. The supernatant fraction was discarded, and DEAE-cellulose was resuspended in buffer containing 20 mM Tris, pH 8.0, and 15 mM 2-mercaptoethanol. The DEAE-cellulose was washed three times by repeated centrifugation and resuspension before being poured into a column for elution. The packed column was washed with buffer until the effluent was free of protein. The adsorbed protein was eluted with 150 mM KCl, 20 mM Tris, pH 8.0, and 15 mM 2-mercaptoethanol and then pooled and lyophilized. The lyophilized powder was resuspended in a minimal volume of 20 mM Mops, pH 7.0, and 15 mM 2-mercaptoethanol and dialyzed against the same buffer to remove salt. A typical yield of mixed light chains was 3 and 1.5 g per kg of skeletal or cardiac muscle, respectively. The P light chain constituted 30–50% of the protein in the mixed light chain fraction as judged by electrophoresis on 10% polyacrylamide gels in the presence of 0.1% sodium dodecyl sulfate. The P light chain could be purified to electrophoretic homogeneity by chromatography of the mixed light chain fraction on DEAE-cellulose as described by Jakes et al. (1976). The resulting mixed light chain fraction was free of detectable calmodulin as judged by the fraction's inability to activate calmodulin-deficient myosin light chain kinase. The phosphate content of the P light chain from skeletal or cardiac muscle was negligible as determined by direct measurement of protein-bound phosphate (Stull & Buss, 1977) and by stoichiometric phosphorylation (to the extent of 1 mol of phosphate/mol of P light chain) after prolonged incubation with myosin light chain kinase.

Calmodulin was prepared by the procedure of Dedman et al. (1977) from frozen bovine brain obtained from Pel-Freez. Calmodulin was coupled to cyanogen bromide activated Sepharose 4B by the method of Klee & Krinks (1978). The molecular weight of calmodulin used for all calculations was 17 000 (Watterson et al., 1980).

Myosin light chain kinase was prepared from back and hind limb skeletal muscle of freshly killed rabbits. The procedure employed affinity adsorption chromatography on calmodulin-Sepharose 4B and was essentially the method described by Yazawa & Yagi (1978). A specific activity of 6.7 μmol of ^{32}P incorporated per min per mg of enzyme was obtained in the presence of saturating concentrations of substrates, Ca^{2+} , and calmodulin. Identical V_{max} values were obtained by using either cardiac or skeletal muscle light chains; the K_{m} values of cardiac and skeletal muscle P light chains were 20 and 10 μM , respectively, in good agreement with previously published results obtained with partially purified skeletal muscle myosin light chain kinase (Stull et al., 1978). These results suggest only minor differences between these protein substrates with regard to phosphorylation by the skeletal muscle kinase. An apparent molecular weight of 90 000 was obtained for myosin light chain kinase by electrophoresis on 5% polyacrylamide gels in the presence of 0.1% sodium dodecyl sulfate. A similar molecular weight was determined by gel filtration under nondenaturing conditions. These physical and enzymatic properties of the purified enzyme are in good agreement with those previously published (Yazawa & Yagi, 1978; Nairn & Perry, 1979).

Protein Determinations. Protein concentrations were determined by a biuret procedure with bovine serum albumin as the standard.

Myosin Light Chain Kinase Assay. Enzyme activity was determined by rates of ^{32}P incorporation into mixed bovine cardiac light chains at 30 °C. Indicated free Ca^{2+} concentrations were either buffered with 3 mM EGTA or represent total Ca^{2+} concentration in those experiments without an EGTA buffer. The EGTA constants previously described (Stull & Buss, 1978) were used to calculate the free Ca^{2+} concentrations in the Ca^{2+} /EGTA-buffered experiments. All reagents and substrates used in the nonbuffered assays were chromatographed on Chelex-100 as previously described (Stull & Buss, 1978) to remove contaminating divalent cations and were stored in plastic containers which had been thoroughly rinsed with deionized water. Because the level of contaminating Ca^{2+} was too low to measure directly by atomic absorption spectrometry, $^{45}\text{Ca}^{2+}$ (10 μM) was added to all materials before Chelex-100 chromatography as described by Stull & Buss (1978). The concentration of contaminating calcium in Chelex-treated solutions as determined by this procedure was 20 nM or less. The cardiac light chains and [γ - ^{32}P]ATP were chromatographed on Chelex-100 twice, the first time in the presence of 1 mM Mg^{2+} to displace any tightly bound Ca^{2+} . Calmodulin was applied to a Chelex column at a high concentration (approximately 5 mg/mL) before dilution into the assay. Ultrapure magnesium salts containing <1 ppm of Ca^{2+} were used in the reaction. A primary standard solution of CaCl_2 was used for Ca^{2+} /EGTA-buffered and nonbuffered experiments. Kinase reactions without a Ca^{2+} /EGTA buffer (Figure 6) were performed in well-rinsed polypropylene tubes. The Ca^{2+} /EGTA-buffered assays (Figures 1 and 2) were performed in 6 \times 50 mm borosilicate glass tubes. Each reaction mixture (50 μL final volume) also contained 50 mM Mops, pH 7.0, 15 mM 2-mercaptoethanol, 10 mM magnesium acetate (except as indicated otherwise), the indicated concentration of mixed cardiac light chains, 16 ng/mL kinase (0.2 nM), 1 mM [γ - ^{32}P]ATP (150–300 cpm/pmol), and the indicated concentrations of calmodulin. The reaction mixtures were incubated for at least 5 min at 30 °C before the reactions were started by addition of ATP. Aliquots (20 μL) of each reaction mixture were removed after 5 and 15 min and spotted on 3 MM filter paper squares. The squares were immediately immersed in 10% trichloroacetic acid and 4% pyrophosphate and processed by the procedure of Corbin & Reimann (1975). Blanks consisting of reaction mixtures with no added kinase contained identical amounts of radioactivity (<200 cpm) as complete assay mixtures containing 3 mM EGTA with no added Ca^{2+} . The radioactivity of 3 mM EGTA blanks was routinely subtracted from the total radioactivity of each determination to calculate initial rates of phosphorylation.

Results

Activation of Myosin Light Chain Kinase by Calmodulin. Figure 1 illustrates the activation of myosin light chain kinase by calmodulin at various fixed concentrations of Ca^{2+} . At low Ca^{2+} concentrations (<1.19 μM), no activity was observed until very high concentrations of calmodulin were reached (>100 nM). As the Ca^{2+} concentration was increased, the enzyme was activated by lower concentrations of calmodulin; i.e., the calmodulin concentration required for half-maximal activation (K_{CMapp}) decreased. At Ca^{2+} concentrations less than 16 μM , small increases in Ca^{2+} concentration resulted in large decreases in the value of K_{CMapp} . However, at Ca^{2+} concentrations greater than 36 μM , large changes in Ca^{2+} concentration caused only slight changes in K_{CMapp} , indicating

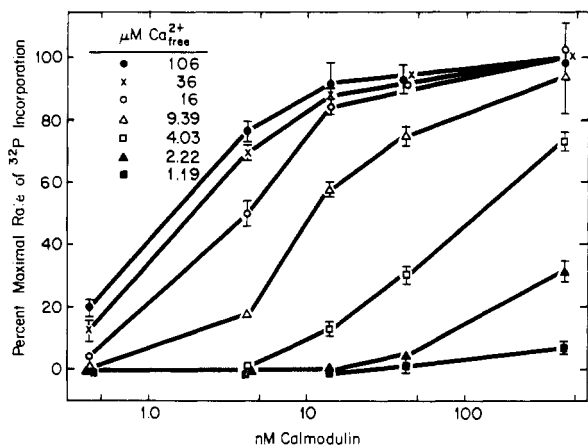


FIGURE 1: Activation of myosin light chain kinase by calmodulin as a function of Ca^{2+} concentration. The rates of ^{32}P incorporation into mixed cardiac myosin light chains were determined as described under Methods and Materials at the indicated concentrations of calmodulin and Ca^{2+} . The P light chain concentration was $6 \mu\text{M}$. The maximal rate of ^{32}P incorporation was calculated as the average of the rates obtained at 420 nM calmodulin and $16, 36$, and $106 \mu\text{M}$ Ca^{2+} . Ca^{2+} concentrations less than or equal to $9.39 \mu\text{M}$ Ca^{2+} were controlled by using a $\text{Ca}^{2+}/\text{EGTA}$ buffer system as described under Methods and Materials. Ca^{2+} concentrations greater than $9.39 \mu\text{M}$ were not buffered by EGTA. Data points indicate the mean \pm SEM of at least four determinations.

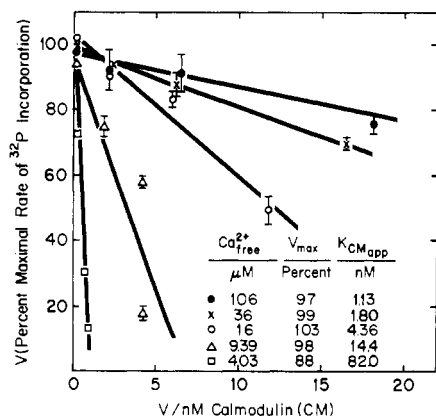


FIGURE 2: Eadie-Hofstee plot of calmodulin activation curves. Values for V_{max} and K_{CMapp} as a function of Ca^{2+} concentration were determined from the vertical axis intercept and the slope, respectively, of each line. Best-fit lines were obtained by least-squares linear regression analysis of the indicated data points from Figure 2.

that at very high Ca^{2+} concentrations ($>100 \mu\text{M}$) K_{CMapp} approaches a minimal value (approximately 1 nM).

These observations are more apparent in Figure 2, where the data are plotted in an Eadie-Hofstee format. Again, K_{CMapp} (as calculated from the best-fit lines) was observed to decrease with increasing Ca^{2+} concentration. The same V_{max} values were obtained for all of the calmodulin activation curves. The Eadie-Hofstee plots also demonstrate that calmodulin activation of myosin light chain kinase follows simple hyperbolic kinetics, as indicated by the linear form of each calmodulin activation curve. When the calmodulin activation curves were analyzed by Hill plots (Figure 3), an average Hill coefficient (n_H) of 0.97 is obtained, again indicating simple hyperbolic kinetics with respect to activation of myosin light chain kinase by calmodulin.

Activation of Myosin Light Chain Kinase by Ca^{2+} . Figure 4 represents a replot of the data in Figure 1, showing myosin light chain kinase activity as a function of Ca^{2+} concentration. At low concentrations of calmodulin ($<0.42 \text{ nM}$), the enzyme required relatively high concentrations of Ca^{2+} ($>16 \mu\text{M}$) for

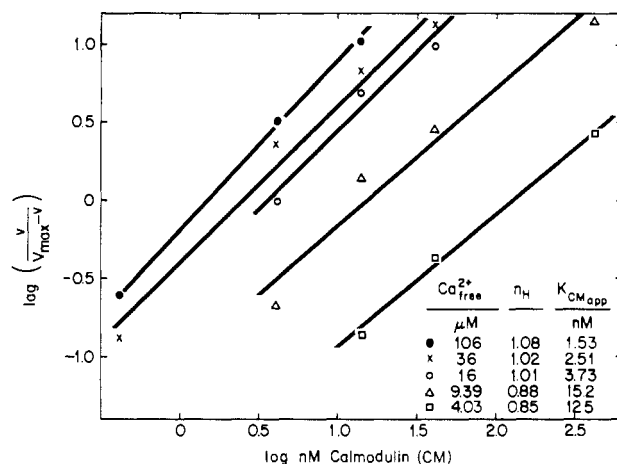


FIGURE 3: Hill plots of calmodulin activation curves. Values for the Hill coefficient (n_H) and K_{CMapp} as a function of Ca^{2+} concentration were determined from the slope and the horizontal axis intercept ($\log [v/(V_{\text{max}} - v)] = 0$), respectively. The same V_{max} value was used in the calculation of position with respect to the vertical axis for all points. Best-fit lines were determined by least-squares linear regression analysis.

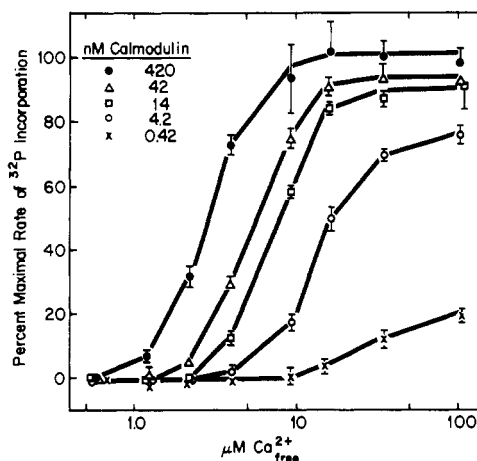


FIGURE 4: Activation of myosin light chain kinase by Ca^{2+} as a function of calmodulin concentration. The data are identical with those in Figure 1, but plotted to illustrate the effect of calmodulin concentration on Ca^{2+} activation.

activity. As the calmodulin concentration in the assay was increased, the enzyme became activated at lower concentrations of Ca^{2+} (i.e., $K_{\text{Ca}^{2+},\text{app}}$ decreased as calmodulin concentration increased). In contrast to the calmodulin activation curves, the apparent V_{max} of a given Ca^{2+} activation curve apparently decreased as the calmodulin concentration was decreased. Analysis of the Ca^{2+} activation curves by means of Hill plots (Figure 5) resulted in Hill coefficients (n_H) of 3 , indicating at least three Ca^{2+} binding sites interact with respect to enzyme activation. Activation by Ca^{2+} at a fixed calmodulin concentration (42 nM) resulted in a marked increase in the V_{max} value for both reaction substrates (ATP and P light chain), but had no effect on the K_m value for either substrate (data not shown). Identical Ca^{2+} activation curves were obtained at P light chain concentrations well below ($6 \mu\text{M}$) and above ($46 \mu\text{M}$) the K_m ($20 \mu\text{M}$) for P light chains (Figure 6). These data suggest that the activation site is spatially distinct from the catalytic site.

Ca^{2+} Activation in the Absence of $\text{Ca}^{2+}/\text{EGTA}$ Buffer and the Effect of Mg^{2+} . Ca^{2+} activation experiments were performed at 42 nM calmodulin with assay materials which had been freed of contaminating divalent metals by Chelex-100

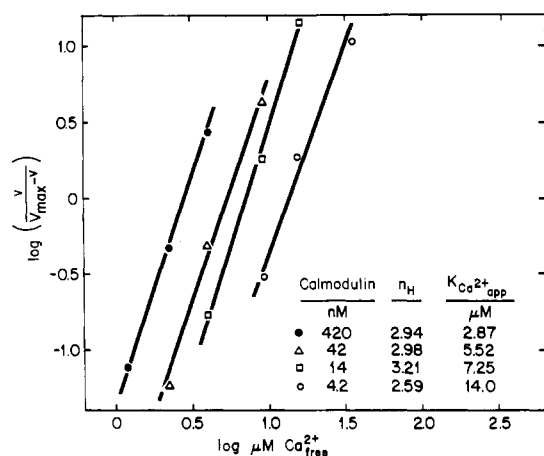


FIGURE 5: Hill plots of Ca^{2+} activation curves. Data from Figure 4 were analyzed to determine values for the Hill coefficient (n_H) and $K_{Ca^{2+} app}$ from the slope and value of $\log [v/(V_{max} - v)] = 0$, respectively, for each Ca^{2+} activation curve. The values of V_{max} used to calculate the position of a given point with respect to the vertical axis were 100, 92, 89, and 76% of the maximal rate for the curves determined at 420, 42, 14, and 4.2 nM calmodulin, respectively. Best-fit lines were determined by least-squares linear regression analysis.

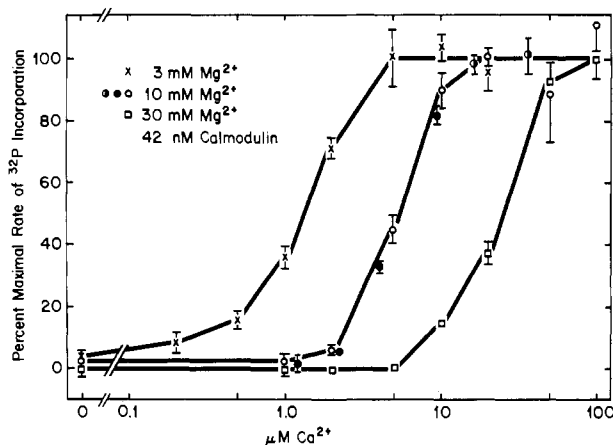
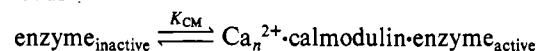
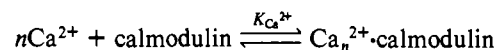


FIGURE 6: The effect of Mg^{2+} concentration on the activation of myosin light chain kinase by Ca^{2+} . Assays were performed without a Ca^{2+} /EGTA buffer system (as described in Methods and Materials) in the presence of 42 nM calmodulin, 46 μM P light chain, and the indicated concentrations of Mg^{2+} . All data are shown normalized to the same maximal rate. The maximal rates of ^{32}P incorporation were not significantly different between the 3 and 10 mM Mg^{2+} curves. The rate obtained at 30 mM Mg^{2+} and 100 μM Ca^{2+} was 90% of the maximal activity observed at the lower Mg^{2+} concentrations. The Ca^{2+} activation curve from Figure 1 obtained with 42 nM calmodulin, 6 μM P light chain, and 10 mM Mg^{2+} is shown by the closed and semiclosed circles, indicating the presence or absence, respectively, of a Ca^{2+} /EGTA buffer system. All data are represented as the mean \pm SEM of at least four determinations.

chromatography (Figure 6) to verify the data obtained by using a standard Ca^{2+} /EGTA buffer system. Identical Ca^{2+} activation curves were obtained at 10 mM Mg^{2+} for both Ca^{2+} /EGTA-buffered and nonbuffered experiments, indicating the Ca^{2+} /EGTA buffer used to control free Ca^{2+} concentration provides reasonably accurate values for the free Ca^{2+} concentration and is not responsible for the steep activation curves observed in Figure 4. Furthermore, it was found that Mg^{2+} competitively inhibits enzyme activation by Ca^{2+} (Figure 6).

Discussion

Mechanistic Model for the Activation of Myosin Light Chain Kinase. The data obtained in the present study suggest the following mechanistic model:



Each equilibrium is fully reversible and follows the laws of mass action. The activation sequence appears to involve (1) occupation of at least three independent Ca^{2+} binding sites on calmodulin to form the complex, $Ca_n^{2+} \cdot \text{calmodulin}$, and (2) interaction of $Ca_n^{2+} \cdot \text{calmodulin}$ with the inactive enzyme catalytic subunit to form the catalytically active holoenzyme complex, $Ca_n^{2+} \cdot \text{calmodulin} \cdot \text{enzyme}$.

Evidence that occupation of at least three Ca^{2+} binding sites on calmodulin is required for activation comes from the Hill analysis of kinase activation by Ca^{2+} (Figure 5). Hill coefficients (n_H) of 3 indicate at least three Ca^{2+} binding sites interact in a positive fashion with respect to activation. Calmodulin is known to have four divalent metal binding sites from studies of the protein's amino acid sequence (Watterson et al., 1980) and from direct equilibrium binding studies (Lin et al., 1974; Watterson et al., 1976; Dedman et al., 1977; Klee, 1977; Wolff et al., 1977). However, the equilibrium binding studies do not indicate any cooperativity between the sites with respect to Ca^{2+} binding. A simple explanation for the apparent positive cooperativity of the Ca^{2+} activation data is that the occupation of several sites by Ca^{2+} is required before calmodulin can activate the enzyme catalytic subunit.

Activation of myosin light chain kinase is specific for Ca^{2+} . No appreciable enzymatic activity is observed at Ca^{2+} concentrations less than 0.1 μM, even in the presence of 10 mM Mg^{2+} (Figure 4). Similarly, the catalytic subunit does not interact with calmodulin-Sepharose 4B in the presence of 2 mM Mg^{2+} if Ca^{2+} is not present (data not shown). Competitive inhibition of Ca^{2+} activation by Mg^{2+} (Figure 6) indicates that Mg^{2+} may displace Ca^{2+} from the divalent metal binding sites and thereby prevent calmodulin interaction with the catalytic subunit.

Formation of the catalytically active holoenzyme at fixed Ca^{2+} concentrations follows simple hyperbolic kinetics (Figures 2 and 3), indicating a 1:1 stoichiometry of interaction between the Ca^{2+} -calmodulin complex and the enzyme catalytic subunit. As illustrated by Figures 1, 2, and 3, $K_{CM app}$ appears to approach a minimum value (approximately 1 nM) at Ca^{2+} concentrations in excess of 100 μM. At these high Ca^{2+} concentrations, essentially all of the Ca^{2+} binding sites on calmodulin would be occupied, and, therefore, $K_{CM app}$ would be equal to the true or intrinsic activation constant for $Ca_n^{2+} \cdot \text{calmodulin}$ (indicated as K_{CM} in the model).

Derivation of the Rate Equation for Myosin Light Chain Kinase Activation. A simple rate equation describing the extent of enzyme activation as a function of Ca^{2+} and calmodulin concentration can be easily derived from the model proposed in the previous section, if it is assumed that the fractional activity (v/V_{max}) is equal to the fraction of total enzyme in the holoenzyme complex. An expression describing Ca^{2+} binding to calmodulin to form the complex, $Ca_n^{2+} \cdot \text{calmodulin}$, is first derived. This equation is then used to describe the formation of the active holoenzyme complex, $Ca_n^{2+} \cdot \text{calmodulin} \cdot \text{enzyme}_{\text{active}}$.

The concentration of $Ca_n^{2+} \cdot \text{calmodulin}$ is given by eq 1 (Segel, 1975). $[CM]$ represents the total concentration of calmodulin, $[Ca^{2+}]$ represents the free Ca^{2+} concentration, and $K_{Ca^{2+}}$ represents the intrinsic activation constant for Ca^{2+} . This equation assumes that n independent, equivalent Ca^{2+} binding sites on calmodulin are involved in enzyme activation and that

$$[Ca_n^{2+} \cdot CM] = \frac{([Ca^{2+}]/K_{Ca^{2+}})^n}{(1 + [Ca^{2+}]/K_{Ca^{2+}})^n} [CM] = \frac{[CM]}{(1 + K_{Ca^{2+}}/[Ca^{2+}])^n} \quad (1)$$

activation cannot occur until these particular sites are occupied by Ca^{2+} . The number of sites which are involved in activation has not been unequivocally established; therefore, a value for n , the apparent number of Ca^{2+} binding sites required to be occupied for activation, will not be assigned at this point in the analysis.

The overall rate equation describing the fractional enzyme activity, v/V_{max} in terms of the Ca^{2+} and calmodulin concentrations is obtained by substituting eq 1 into an equation analogous to the Michaelis-Henri equation (eq 2-4). Use

$$v/V_{max} = [Ca_n^{2+} \cdot CM] / (K_{CM} + [Ca_n^{2+} \cdot CM]) \quad (2)$$

$$v/V_{max} = [CM] (1 + K_{Ca^{2+}}/[Ca^{2+}])^{-n} / [K_{CM} + [CM] \times (1 + K_{Ca^{2+}}/[Ca^{2+}])^{-n}] \quad (3)$$

$$v/V_{max} = [CM] / [K_{CM} (1 + K_{Ca^{2+}}/[Ca^{2+}])^n + [CM]] \quad (4)$$

of this equation was suggested by the simple hyperbolic kinetics observed with respect to calmodulin activation. The implicit assumption is made that only Ca_n^{2+} -calmodulin can activate the catalytic subunit. The overall rate equation assumes rapid equilibrium conditions, i.e., that the kinase catalytic subunit concentration is much less than K_{CM} (the intrinsic activation constant of Ca_n^{2+} -calmodulin for the enzyme), and that the rate of formation of the reaction product (phosphorylated myosin light chain) is not limited by the rate of formation of Ca_n^{2+} -calmodulin-enzyme. These conditions were satisfied in the activation experiments. The concentration of enzyme in each reaction was 0.2 nM, sufficiently below the estimated K_{CM} (~ 1 nM) to satisfy the first condition. The reaction mixtures were equilibrated for at least 5 min before the reactions were started to allow sufficient time for the holoenzyme complex to come to equilibrium. Linear rates of phosphorylation were observed in every reaction, indicating equilibrium had been reached.

Determination of K_{CM} , $K_{Ca^{2+}}$, and n . The use of eq 4 to predict the extent of enzyme activation, v/V_{max} , depends on the appropriate choice of values for the constants $K_{Ca^{2+}}$, K_{CM} , and n . These can be determined from the data by expressing eq 4 in a form that can be plotted as a line. When terms in eq 4 are rearranged

$$[CM](V_{max}/v) = K_{CM}(1 + K_{Ca^{2+}}/[Ca^{2+}])^n + [CM] \quad (5)$$

$$[CM](V_{max}/v - 1) = K_{CM}(1 + K_{Ca^{2+}}/[Ca^{2+}])^n \quad (6)$$

and roots taken

$$[[CM](V_{max}/v - 1)]^{1/n} = (K_{CM})^{1/n} (1 + K_{Ca^{2+}}/[Ca^{2+}]) \quad (7)$$

$$[[CM](V_{max}/v - 1)]^{1/n} = (K_{CM})^{1/n} + (K_{CM})^{1/n} K_{Ca^{2+}} ([Ca^{2+}])^{-1} \quad (8)$$

an equation is obtained which can be plotted as $[Ca^{2+}]^{-1}$ vs. $[[CM](V_{max}/v - 1)]^{1/n}$. The value of n is determined by the plot which yields a straight line. The vertical axis intercept represents the n th root of K_{CM} , whereas $K_{Ca^{2+}}$ is determined from the negative reciprocal of the horizontal axis intercept.

Figure 7 illustrates the results of this analysis by using the data plotted in Figure 1. When values of $n = 2$ or 3 are used to calculate the position of each data point with respect to the vertical axis, the curve is clearly concave upward, while values of n greater than 4 yield curves which are concave downward. The curve resulting from $n = 4$ is a straight line, indicating

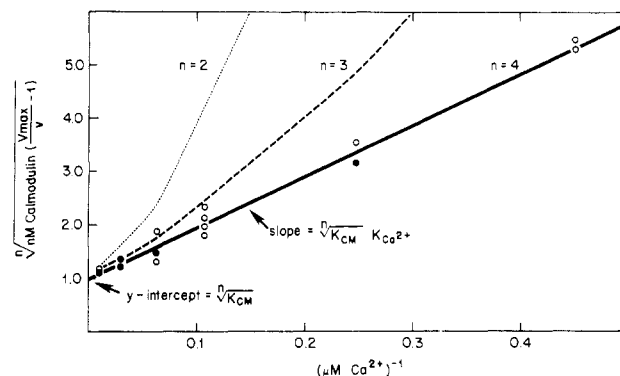


FIGURE 7: Determination of n , K_{CM} , and $K_{Ca^{2+}}$. Data from Figure 1 are plotted as described in the Discussion. Values calculated with $n = 4$ are represented by symbols; (O) one point, (●) two points. (—) represents the best-fit line when $n = 4$ as determined by least-squares linear regression. The curves determined by $n = 2$ (---) and $n = 3$ (---) as indicated (individual data points for $n = 2$ and $n = 3$ are not represented). All data points from Figures 1 and 4 are represented except those within 3% of 0 and 100% maximal rate of ^{32}P incorporation. The data point from $1.19 \mu M$ Ca^{2+} and 420 nM calmodulin falls directly on the heavy solid line (—) when $n = 4$, but is outside the boundaries of the plot.

that the number of sites Ca^{2+} must occupy before activation can occur appears to be four. The values obtained from the plot when $n = 4$ for K_{CM} and $K_{Ca^{2+}}$ are 0.86 nM and $10 \mu M$, respectively. These values are in reasonable agreement with those previously published for myosin light chain kinase (Yazawa & Yagi, 1978; Nairn & Perry, 1979) and other calmodulin-dependent enzyme systems (see reviews by Wolff & Brostrom, 1979; Wang & Waisman, 1979; Cheung, 1980; Klee et al., 1980).

The plot in Figure 7 clearly indicates that only the Ca_4^{2+} -calmodulin complex interacts with the enzyme to an appreciable extent. If, for example, Ca_3^{2+} -calmodulin (as well as Ca_4^{2+} -calmodulin) bound to the enzyme with an affinity equal to or greater than that for Ca_4^{2+} -calmodulin, then nonlinear curves would result when $[[CM](V_{max}/v - 1)]^{1/4}$ vs. $[Ca^{2+}]^{-1}$ is plotted. Nonlinear plots would occur whether Ca_3^{2+} -calmodulin binding resulted in activation or prevented activation by Ca_4^{2+} -calmodulin. If the affinity of the enzyme for Ca_3^{2+} -calmodulin was at least 10-fold lower than that for Ca_4^{2+} -calmodulin, then Ca_3^{2+} -calmodulin would not exert a measurable effect on the enzyme activity, and linear plots would result. Similar arguments can be made regarding Ca_1^{2+} -calmodulin and Ca_2^{2+} -calmodulin. Thus, calmodulin complexes with less than four sites occupied by Ca^{2+} may be capable of binding to myosin light chain kinase, but do not have a significant effect on the extent of enzyme activation by Ca_4^{2+} -calmodulin.

Figure 8 illustrates the fit of the data to eq 4 with the values for $K_{Ca^{2+}}$, K_{CM} , and n determined from Figure 7. The equation and constants fit the data quite well over the wide range of Ca^{2+} and calmodulin concentrations which were studied. The largest variation between the data and the model (an absolute difference of 13% of the maximal rate) is obtained at 14 nM calmodulin and $16 \mu M$ Ca^{2+} and probably represents experimental variability.

Previous kinetic models differ from the present model primarily with respect to the number of Ca^{2+} binding sites on calmodulin required for enzyme activation. Yazawa et al. (1978) proposed that myosin light chain kinase required binding of two molecules of Ca^{2+} to calmodulin for activation. Wolff et al. (1977) suggested three Ca^{2+} binding sites were involved in the activation of cyclic nucleotide phosphodi-

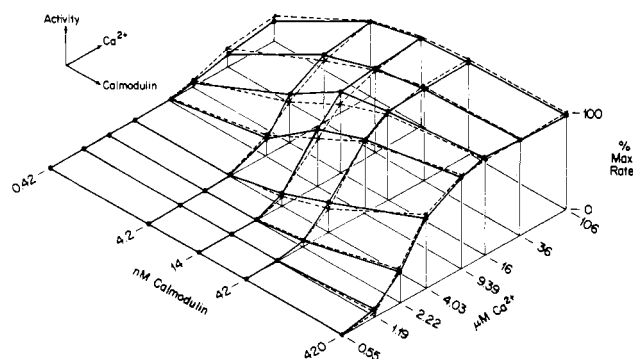


FIGURE 8: Myosin light chain kinase activity surface. Activity is plotted on the vertical axis as a function of Ca^{2+} and calmodulin concentration (as indicated on the horizontal axes). The solid lines represent the data from Figures 1 and 4. The dotted lines connect the corresponding points calculated from eq 4 by using the kinetic constants determined from Figure 7.

esterase. Dedman et al. (1977) proposed that activation of phosphodiesterase occurs as the result of Ca^{2+} binding to any one of four equivalent sites on calmodulin. These previous models were all based on Ca^{2+} binding properties and particularly Ca^{2+} activation data obtained at a single calmodulin concentration. The present kinetic analysis demonstrates the importance of using enzyme activation data obtained over a wide range of Ca^{2+} and calmodulin concentrations for the development of a kinetic model and determination of kinetic parameters.

It should be noted that the constants $K_{\text{Ca}^{2+}}$ and K_{CM} are not true dissociation constants, but rather intrinsic activation constants. Allosteric effectors are commonly thought to act by directly or indirectly changing the equilibrium between various conformational states of an enzyme or protein (Monod et al., 1965; Koshland et al., 1966). If transitions between various conformational states of calmodulin and the catalytic subunit occur during activation, then the activation constants $K_{\text{Ca}^{2+}}$ and K_{CM} will represent equilibrium constants comprised of equilibrium dissociation and transitional constants. A more thorough kinetic analysis is required before the present model can be elaborated to include possible transition equilibria. Furthermore, the value of the constants also depends on the validity of the assumptions made when developing the rate equation. For example, it was assumed that $K_{\text{Ca}^{2+}}$ was the same for each Ca^{2+} binding site. In actuality, $K_{\text{Ca}^{2+}}$ represents an average activation constant for the four apparent Ca^{2+} binding sites, which may or may not bind Ca^{2+} with exactly the same affinity.

A large number of physicochemical studies indicate that as Ca^{2+} binds to calmodulin the protein undergoes marked structural changes (reviewed by Wolff & Brostrom, 1979; Wang & Waisman, 1979; Cheung, 1980; Klee et al., 1980). The present study is the first to indicate that the conformation of calmodulin which activates myosin light chain kinase is Ca_4^{2+} -calmodulin. In light of the evidence that calmodulin is highly conserved with respect to structure and function throughout eukaryotic evolution, it is interesting to speculate that the evolutionary pressure which has maintained the protein's primary structure is the requirement that calmodulin have four molecules of Ca^{2+} bound before it can regulate any given calmodulin-dependent process. Analysis of the activation of other calmodulin-dependent enzymes by the methods outlined in this paper should prove useful in substantiating this hypothesis.

In summary, the kinetic model for the activation of myosin light chain kinase by Ca^{2+} and calmodulin represents the first

description which accurately predicts the extent of enzyme activation over a wide range of Ca^{2+} and calmodulin concentrations. The data were analyzed by a technique which determined the apparent number of Ca^{2+} binding sites involved in activation as well as values for the kinetic constants K_{CM} and $K_{\text{Ca}^{2+}}$. The techniques employed in the analysis of myosin light chain kinase activation should be generally applicable to other enzymes dependent on Ca^{2+} and calmodulin for activation.

References

- Barylko, B., Kuznicki, J., & Drabikowski, W. (1978) *FEBS Lett.* 90, 301-304.
- Brostrom, C. O., & Wolff, D. J. (1974) *Arch. Biochem. Biophys.* 165, 715-727.
- Cheung, W. Y. (1980) *Science (Washington, D.C.)* 207, 19-27.
- Corbin, J. D., & Reimann, E. M. (1975) *Methods Enzymol.* 38, 287-290.
- Dabrowska, R., Aromatorio, D., Sherry, J. M. F., & Hartshorne, D. J. (1977) *Biochem. Biophys. Res. Commun.* 78, 1263-1272.
- Dabrowska, R., Sherry, J. M. F., Aromatorio, D. K., & Hartshorne, D. J. (1978) *Biochemistry* 17, 253-258.
- Dedman, J. R., Potter, J. D., Jackson, R. L., Johnson, J. D., & Means, A. R. (1977) *J. Biol. Chem.* 252, 8415-8422.
- Jakes, R., Northrop, F., & Kendrick-Jones, J. (1976) *FEBS Lett.* 70, 229-234.
- Klee, C. B. (1977) *Biochemistry* 16, 1017-1024.
- Klee, C. B., & Krinks, M. M. (1978) *Biochemistry* 17, 120-126.
- Klee, C. B., Crouch, T. H., & Richman, P. G. (1980) *Annu. Rev. Biochem.* 49, 489-515.
- Koshland, D. E., Jr., Nemeny, G., & Filmer, D. (1966) *Biochemistry* 5, 365-385.
- Lin, Y. M., Liu, Y. P., & Cheung, W. Y. (1974) *J. Biol. Chem.* 249, 4943-4954.
- Monod, J., Changeux, J.-P., & Jacob, F. (1964) *J. Mol. Biol.* 12, 88-118.
- Nairn, A. C., & Perry, S. V. (1979) *Biochem. J.* 179, 89-97.
- Pires, E. M. V., & Perry, S. V. (1977) *Biochem. J.* 167, 137-146.
- Pires, E., Perry, S. V., & Thomas, M. A. W. (1974) *FEBS Lett.* 41, 292-296.
- Segel, I. H. (1975) *Enzyme Kinetics: Behavior and Analysis of Rapid Equilibrium and Steady-State Enzyme Systems*, p 357, Wiley, New York.
- Solaro, R. J., Pang, D. C., & Briggs, F. N. (1971) *Biochim. Biophys. Acta* 245, 259-262.
- Stull, J. T., & Buss, J. E. (1977) *J. Biol. Chem.* 252, 851-857.
- Stull, J. T., & Buss, J. E. (1978) *J. Biol. Chem.* 253, 5932-5938.
- Stull, J. T., Blumenthal, D. K., deLanerolle, P., High, C. W., & Manning, D. R. (1978) *Adv. Pharmacol. Chemother.* 3, 171-180.
- Teo, T. S., & Wang, J. H. (1973) *J. Biol. Chem.* 248, 5950-5955.
- Walsh, M. P., Vallet, B., Autric, F., & Demaille, J. G. (1979) *J. Biol. Chem.* 254, 12136-12144.
- Wang, J. H., & Waisman, D. M. (1979) *Curr. Top. Cell. Regul.* 15, 47-107.
- Watterson, D. M., Harrelson, W. G., Keller, P. M., Sharief, F., & Vanaman, T. C. (1976) *J. Biol. Chem.* 251, 4501-4513.
- Watterson, D. M., Sharief, F., & Vanaman, T. C. (1980) *J. Biol. Chem.* 255, 962-975.

- Wolff, D. J., & Brostrom, C. O. (1979) *Adv. Cyclic Nucleotide Res.* 11, 27-88.
- Wolff, D. J., Poirier, P. G., Brostrom, C. O., & Brostrom, M. A. (1977) *J. Biol. Chem.* 252, 4108-4117.
- Yagi, K., Yazawa, M., Kakiuchi, S., Oshima, M., & Uenishi, K. (1978) *J. Biol. Chem.* 253, 1338-1340.

- Yazawa, M., & Yagi, K. (1977) *J. Biochem. (Tokyo)* 82, 287-289.
- Yazawa, M., & Yagi, K. (1978) *J. Biochem. (Tokyo)* 84, 1259-1265.
- Yazawa, M., Kuwayama, H., & Yagi, K. (1978) *J. Biochem. (Tokyo)* 84, 1253-1258.

Effects of Actin and Calcium Ion on Chymotryptic Digestion of Skeletal Myosin and Their Implications to the Function of Light Chains[†]

Steven Oda, Christine Oriol-Audit,[‡] and Emil Reisler*

ABSTRACT: Experiments have been carried out to assess the involvement of the myosin light chains [obtained by treatment of myosin with 5,5'-dithiobis(2-nitrobenzoic acid) (Nbs₂)] in the control of cross-bridge movement and actomyosin interactions. Chymotryptic digestions of myosin, actomyosin, and myofibrils do not detect any Ca²⁺-induced change in the subfragment 2 region of myosin. Actin, like Ca²⁺, protects the in situ Nbs₂ light chains from proteolysis and causes a partial switch in the digestion product of myosin from subfragment 1 to heavy meromyosin. This effect is independent of the state of aggregation of myosin, and it persists in acto heavy meromyosin and in actomyosin in 0.6 M NaCl. Di-

gestions and sedimentation studies indicate that there is no direct acto light chain interaction. Proteolysis of myosin shows a gradual transition from production of heavy meromyosin to subfragment 1 with lowering of the salt level. In the presence of Ca²⁺ heavy meromyosin is generated both in digestions of polymeric and of monomeric myosin. These results are explained in terms of localized changes within the Nbs₂ light chains and subfragment 1. Subunit interactions in the myosin head lead to a Ca²⁺-induced reduction in the affinity of heavy meromyosin for actin in the presence of MgATP. The resulting Ca²⁺ inhibition of the actin-activated ATPase of myosin can be detected at high salt concentrations (75 mM KCl).

The movement of myosin cross bridges is a central feature in all of the theories of muscular contraction (Huxley, 1969; Huxley & Simmons, 1971; Eisenberg & Hill, 1978; Harrington, 1979a). The nature and the mechanical consequences of this movement have not been yet fully elucidated. In the Huxley model (Huxley, 1969), the action of the cross bridges is linked to a "swinging away" of the subfragment-2 (S-2)¹ region of myosin from the backbone of the thick filament. A transient release of the S-2 region is similarly postulated in the helix-coil model of force generation in muscle (Harrington, 1971, 1979a). Several studies support the view that some conformational changes occur in the thick filament when Ca²⁺ binds to the associated Nbs₂ chains. These Ca²⁺-induced changes were detected by hydrodynamic experiments with thick filaments (Morimoto & Harrington, 1974) and X-ray diffraction studies with striated muscle (Haselgrove, 1975; Huxley, 1979). The binding of Ca²⁺ also appears to significantly weaken actomyosin interactions (Margossian et al., 1975). The most striking Ca²⁺ effect is revealed in the chymotryptic digestions of polymeric myosin. Subfragment 1 is produced in the absence of divalent cations, and heavy meromyosin, in their presence (Weeds & Taylor, 1975; Weeds & Pope, 1977). These and other observations form a basis for a speculation that the Nbs₂ light chains could be involved in the structural regulation of the myosin cross-bridge movement (Haselgrove, 1975; Harrington, 1979b). However, more direct tests of the mobility and disposition of myosin heads with respect to the thick filament backbone do not confirm a specific

Ca²⁺-induced action (Mendelson & Cheung, 1976; Sutoh & Harrington, 1977). Also, more recent work of Srivastava et al. (1980) does not detect any involvement of the Nbs₂ light chains in the generation of tension by actomyosin threads.

The best documented function of myosin light chains is the modulation of the actin-activated MgATPase in invertebrate muscles (Kendrick-Jones et al., 1976). No equivalent Ca²⁺ sensitivity has been found in vertebrate skeletal muscle. However, activity measurements in solvents approaching physiological ionic strengths may produce a different picture. Thus, removal of the Ca²⁺ binding subunit from cardiac myosin results in an increase in actin-activated ATPase at elevated salt concentrations (Malhotra et al., 1979). In rabbit myofibrils, free of troponin and tropomyosin, Ca²⁺ activation of the MgATPase activity has been detected in solutions containing more than 80 mM KCl (Lehman, 1978). This suggested that perhaps in the typical assays, at low ionic concentrations, the affinity of myosin for actin overrides the Ca²⁺ dependence (Lehman, 1978).

In this work we have attempted to reconcile some of the seemingly inconsistent observations related to the function of the Nbs₂ light chains by investigating the interrelationship between actin and the myosin heavy and light chains. Chymotryptic digestions of myosin, acto heavy meromyosin, actomyosin, and myofibrils revealed a significant actin-induced

[†] From the Department of Chemistry and the Molecular Biology Institute, University of California, Los Angeles, California 90024. Received April 22, 1980. This work was supported by U.S. Public Health Service Grant AM 22031.

[‡] Permanent address: Biochimie Cellulaire, College de France, 75231 Paris, Cedex 05.

¹ Abbreviations used: ATPase, adenosine triphosphatase; Nbs₂ (DTNB in figures) light chain, 19 000 molecular weight subunit of myosin dissociated by treatment with 5,5'-dithiobis(2-nitrobenzoic acid); HMM, heavy meromyosin; S-1, subfragment 1; S-2, subfragment 2; EGTA, ethylene glycol bis(β-aminoethyl ether)-N,N'-tetraacetic acid; DTE, dithioerythritol; ATP, adenosine 5'-triphosphate; EDTA, ethylenediaminetetraacetic acid; Tris, 2-amino-2-(hydroxymethyl)-1,3-propanediol; Bis-Tris, 2-[bis(2-hydroxyethyl)amino]-2-(hydroxymethyl)-1,3-propanediol.